IBRO Neuroscience Reports 10 (2021) 75–82

Contents lists available at ScienceDirect

IBRO Neuroscience Reports

journal homepage: www.sciencedirect.com/journal/IBRO-Neuroscience-Reports

Research Paper

Proliferation rate and differentiation potential are independent during the transition from neurogenesis to gliogenesis in the mouse embryonic spinal cord

Leonora Olivos-Cisneros [a,b,*,1], Jesús Ramírez-Santos [b], Gabriel Gutiérrez-Ospina [b,**]

[a] Programa de Doctorado en Ciencias Biomédicas, Universidad Nacional Autónoma de México, 04510, Mexico
[b] Laboratorio de Biología de Sistemas, Departamento de Biología Celular y Fisiología, Instituto de Investigaciones Biomédicas, Universidad Nacional Autónoma de México, Ciudad de México, 04510, Mexico

ARTICLE INFO

Keywords:
Cell cycle
Gliogenesis
Neurogenesis
Neurosphere culture
Spinal cord

ABSTRACT

Neural stem cells (NSC) restrict their differentiation potential as the central nervous system develops. Experimental evidence suggests that the mechanisms governing the transition from the neurogenic to the gliogenic phase irreversibly affect the ability of NSC to generate neurons. Cell cycle regulation has been associated with cell fate in different models. In this work, we assessed the temporal correlation between the loss of the neurogenic potential and cell cycle lengthening of NSC obtained from embryonic mouse spinal cords, during the transition of the neurogenic to the gliogenic phase, using neurospheres. We also used the cell cycle inhibitor Olomoucine to increase cell cycle length by decreasing the proliferation rate. Our results show that neurospheres obtained from a neurogenic stage give rise mostly to neurons, whereas those obtained from later stages produce preferentially glial cells. During the transition from neurogenesis to gliogenesis, the proliferation rate dropped, and the cell cycle length increased 1.5 folds, as monitored by DNA BrdU incorporation. Interestingly, Olomoucine-treated neurogenic-neurospheres display a reduced proliferation rate and preserve their neurogenic potential. Our results suggest that the mechanisms that restrict the differentiation potential of NSC are independent of the proliferation control.

1. Introduction

During prenatal development, Neural Stem Cells (NSC) undergo a series of symmetrical divisions that expand, asynchronously, NSC pools throughout distinct regions of the central nervous system (CNS). Once the NSC expansion phase ends in each region, asymmetric divisions follow and originate, during several rounds, neural progenitors committed to produce neuroblasts. By the end of neurogenesis, neural progenitors become compromised to generate glioblasts (Qian et al., 2000; Temple, 2006). In most of the developing central nervous system, this transition ends with the ability of NSC to produce neurons (Miller and Gauthier, 2007). Hence, the transition from neuron to glia production may hold clues on the cellular processes underlying the restriction of the NSC neurogenic potential. In this regard, it is well known that this transition is modulated by the interplay of extracellular signals and transcription factors that regulate the expression of specific cell-linage genes (Christie et al., 2013). Nevertheless, the manipulation of these signaling cascades does not lead to the full recovery of NSC neurogenic potential (He et al., 2009; Martens et al., 2002; Seaberg et al., 2005; Whittemore et al., 1999). Understanding the mechanisms that regulate neurogenesis in vivo, can lead to the design of new therapies to promote neural repair after injury (as reviewed by Ruddy and Morshead (2018)) or treatment for pathologies that impair the functioning of NSC during development, like parasitic infections (Bottari et al., 2019; Fracasso et al., 2019). Many of these studies have focus on the telencephalic NSC, in this work we focus on the differentiation potential of the spinal cord because of the biomedical relevance of this tissue.

A mechanistic possibility to explain the loss of NSC neurogenic

* Corresponding author at: Programa de Doctorado en Ciencias Biomédicas, Universidad Nacional Autónoma de México, 04510, Mexico.
** Corresponding author.
E-mail addresses: lolivos@rockefeller.edu (L. Olivos-Cisneros), ramirezs@iibiomedicas.unam.mx (J. Ramírez-Santos), gabo@iibiomedicas.unam.mx (G. Gutiérrez-Ospina).
[1] Current address: Laboratory of Social Evolution and Behavior, The Rockefeller University, New York 10065, United States.

https://doi.org/10.1016/j.ibneur.2020.11.004
Received 1 December 2019; Accepted 25 November 2020

Abbreviations

CNS	Central nervous system
NSC	Neural stem cells
MAP2	Microtubule associated protein 2
GFAP	Glial fibrillary acidic protein
DAPI	4′,6-diamidino-2-phenylindole
E11	Embryonic day 11
E14	Embryonic day 14
P1	Postnatal day 1
CDK	Cyclin dependent kinases
CKI	CDK inhibitors
ARF	Alternative reading frame
INK4	Inhibitor of CDK4
Cip	CDK interacting protein
Kip	Kinase inhibitor protein

potential comes from studies on the regulation of cell cycle. The lengthening of cell cycle (particularly the G1 phase) by inhibiting cyclin-dependent kinases (CDK) 1 and 2, has been shown to induce a premature onset of neurogenesis in the ventral mesencephalon and rostral telencephalon of whole embryo cultures (Calegari and Huttner, 2003). Conversely, if the lengthening of G1 is inhibited, the neurogenic phase gets delayed and the expansion of NSC increases (Lange et al., 2009). It is known that the cell cycle length is variable, depending on the position within the neural tube and the age of the embryo. A thorough characterization of the neural tube growth and specification shows that the proliferation rate decreases, and the cell cycle lengthens, once the neuronal differentiation starts in mouse and chicken embryos (Kicheva et al., 2014). Given that cell cycle lengthening participates on the transition of NSC from the expansion phase to neurogenesis, it is possible that a similar process takes place between neurogenesis and gliogenesis, when the neurogenic potential is lost throughout the developing CNS.

During brain development, the $p19^{ARF}$-p53 signaling pathway regulates the transition from neurogenesis to gliogenesis in telencephalic NSC. Indeed, $p19^{ARF}$ overexpression decreases neurogenesis and promotes glial cell generation by increasing the NSC responsiveness to gliogenic signals (e.g., CNTF); downstream $p19^{ARF}$, p53 decreases NSC self-renewal by inhibiting Myc activity, thus allowing the progression of gliogenesis (Nagao et al., 2008). In addition, downstream p53, some cyclin-dependent kinases inhibitors (CKI) might be upregulated, lengthening the cell cycle and allowing the neurogenesis to gliogenesis transition to occur. This last possibility has not been explored in the spinal cord. The likelihood of it, however, is supported by evidence showing that, during spinal cord development, the three members of the Cip/Kip family of CKI are expressed during neurogenesis; the expression of at least one of them regulates the timing of the cell cycle exit in differentiating neurons (Gui et al., 2007). Hence, this work was set out to address whether the onset of gliogenesis and the loss of NSC neurogenic potential are associated with the lengthening of the NSC cycle in response to the accumulation of cell cycle inhibitors in the spinal cord of mouse embryos.

2. Materials and Methods

2.1. Animals

CD1 mouse embryos and newborn male and female mice were used to conduct the experiments described below. Embryos were obtained through caesarean sections performed to timed pregnant females at embryonic days 11 and 14 (E11 and E14). Newborns were sacrificed within the first 24-to-36 h, at postnatal day 1 (P1) of having been born. Pregnant or parturient females were all kept under regular housing conditions (12/12-dark/light cycles, controlled temperature and humidity) at the animal facility of the Instituto de Investigaciones Biomédicas (IIB), Universidad Nacional Autónoma de México (UNAM). Animal handing and experimental protocols were revised and approved by the Animal Rights Committee at IIB, UNAM.

2.2. Neurosphere cultures

Neurospheres were produced from the cervical segment of the spinal cord dissected from E11, E14 and P1 mice. Cervical spinal cords were collected in pools (n = 5) and incubated 20 min at 37 °C in embryonic digestion solution (0.1% trypsin diluted in versene) or postnatal digestion solution (trypsin (1.33 mg/mL), hyaluronidase (0.67 mg/mL), kynurenic acid (0.2 mg/mL) and DNAse (0.02 mg/mL) diluted in artificial cerebrospinal fluid); the embryonic tissue digestion was inactivated with 10% Fetal Bovine Serum (FBS) diluted in versene and the postnatal tissue digestion with 0.7 mg/mL of trypsin inhibitor. Then, the samples were mechanically dissociated. The resultant cell suspensions were centrifuged at 3000 rpm for 5 min at room temperature and the pellet was then re-suspended in culture media (Dulbecco's modified Eagle's medium (DMEM) and F12 (1:1 v/v supplemented with 25 μg/mL insulin, 100 μg/mL transferring, 20 nM progesterone, 60 μM putrescine, 30 nM sodium selenite, 1 μg/mL heparin and 1× Glutamax supplement). Cells were plated at a density of 250,000 cells/mL and maintained at 37 °C, 5% CO_2. The culture was supplemented with 20 ng/mL FGF2 and 20 ng/mL EGF on days 1, 3, 5 and 7. Secondary neurospheres were obtained from 7 days old, primary neurospheres disaggregated with a solution containing trypsin (0.025%) diluted in versene for 10 min at 37 °C; the disaggregation was inactivated with 10% FBS. Secondary neurospheres were kept in culture for 7 days following the protocol described previously, except for the initial plating density (50,000 cells/mL).

2.3. Neurosphere staining and measurement

To induce cell adhesion and differentiation, neurospheres were harvested and seed onto poly-L-lysine treated coverslips for 48 h at 37 °C, 5% CO_2 and fixed with buffered paraformaldehyde (2%) for 30 min at room temperature. After a thorough wash with phosphate buffer-saline (PBS; 0.1 M, pH 7.4), neurospheres were treated with 0.2% Triton X-100, 1% glycine and 10% horse serum diluted in PBS for 20 min at room temperature, and then incubated with a mixture of primary polyclonal antibodies raised in rabbit against MAP2 (1:500, AB5622, Millipore) and raise in chicken against GFAP (1:500, AB5541, Millipore) during 2 h at room temperature. After three PBS rinses, neurospheres were incubated with a mixture of secondary polyclonal antibodies raised in donkey against chicken (biotin conjugated) and against rabbit (Alexa 594 conjugated) for 90 min; finally, they were incubated with fluorescent avidin for 60 min at room temperature. Neurospheres were counterstained with DAPI and the coverslips carrying them mounted on microscope glass slides using anti-fading mounting medium (Dako). These preparations were used to acquire digital images on a Nikon confocal laser scanning microscope or an Olympus disc spinning unit microscope. The diameter (or the short axis in non-spherical neurospheres) was measured using ImageJ software (NIH) at the middle focal plane.

2.4. Cumulative BrdU incorporation and cell cycle length estimate

Secondary neurosphere cultures (n = 3 per exposure time) were prepared as described above and BrdU (5 μM) was added during the last 1, 3, 6, 12, or 24 h before being collected (i.e. all exposure times were collected at the same time, on day seven of culture). After BrdU exposure, neurospheres were harvested and disaggregated to a single cell suspension that was seeded on poly-L-lysine treated coverslips at a density of 1000 cell/μl. After a 2 h incubation at 37 °C, 5% CO_2, cells were then fixed with 2% paraformaldehyde for 30 min, as described above. For BrdU immunodetection, fixed cells were sequentially treated

with 0.5 N HCl for 20 min at 37 °C, 0.1 M Sodium Borate for 10 min, PBS for 10 min and 0.2% Triton X-100 for 20 min at room temperature. Then, they were incubated with the primary polyclonal antibody raised in mouse against BrdU (1:500, Roche Applied Science) for 2 h at room temperature. After three PBS rinses, cells were incubated with a secondary polyclonal antibody raised in donkey against mouse IgGs conjugated to Alexa 488 for 90 min at room temperature. Finally, cells were counter-stained with DAPI and the coverslips were mounted as described above. These preparations were imaged with an Olympus disc spinning unit microscope. Ten sites per exposure time from separate cultures were imaged using the Systematic Random Sampling tool of the Stereo Investigator software (MBF Bioscience). The proportion of BrdU and DAPI stained nuclei was determined to estimate the cell cycle length using a regression analysis of the active portion of the labeling curve of each age, as described before (Kippin et al., 2005).

2.5. CKI mRNA expression levels

Seven-day-old cultured, secondary neurospheres from four different cultures per age, were harvested and disaggregated to a single cell suspension as previously described. One million cells per condition were rapidly frozen and stored at − 80 until used. When thawed for extraction, the cells were re-suspended in Trizol and the RNA was extracted following protocol recommended by the supplier (Invitrogen). RNA concentration was determined using a NanoDrop and cDNA was synthesized using High Capacity cDNA Reverse Transcription kit (Applied Biosystems). The following sense and antisense primers were used for RT-PCR: $p19^{ARF}$, TGAAGTTCGTGCGATCCCGG and TGAGCAGAAGAGCTGCTACG (160 bp), $p19^{INK4D}$, TCCCCATCCATCTGGCGATA and ATGGCTGTTGCCTGTAGGAG (400 bp), $p16^{INK4A}$, TCACACGACTGGGCGATTG and AGCTCTGCTCTTGGGATTGG (79 bp), $p21^{Cip}$, GGAACATCTCAGGGCCGAAA and CTGAGGATCACCCCCAGGTA (519 bp), $p27^{Kip}$, AGATACGAGTGGCAGGAGGT and TGTTTACGTCTGGCGTCGAA (381 bp), p53 ATTCAGGCCCTCATCCTCCT and GAAGCCATAGTTGCCCTGGT. Actin was used as an internal control. Amplification was accomplished by incubating 100 ng of the cDNA in a 20 µl reaction volume by using 20 pmoles of specific sense and antisense primers and Kapataq Ready mix DNA polymerase (KAPA BIOSYSTEMS) using following conditions: 2 min at 94 °C; 25 cycles of 30 s at 95 °C, 30 s at 55 °C, and 1 min at 72 °C; and 5 min at 72 °C. PCR products were separated by electrophoresis in 2% agarose gels. We quantify the expression levels of each mRNA as the ratio of the Mean Gray Value of the band that each of them displayed on the gel, relative to the loading control. The Mean Gray Value determinations were made with ImageJ software (NIH).

2.6. Olomoucine treatment

Olomoucine is a specific inhibitor of G1 cyclin-dependent kinases that lengthens the cell cycle of neuroepithelial cells. It was added to the culture medium of secondary neurospheres from embryonic day 11 to a final concentration of 50 µM (from a 50 mM stock in DMSO). The same volume of DMSO was added to the control cultures. The neurospheres were collected at day seven of culture, fixed, stained and measured as described above.

2.7. Statistics

Data analyses were carried out with GraphPad Prism 8 (GraphPad Software Inc., La Jolla, CA, USA). Data are given as means plus/minus standard errors. Statistical comparisons of neurosphere diameter between ages and treatments were done with one-way ANOVA test followed by a Tukey's post hoc analysis. The Kruskal–Wallis test was used to compare CKI mRNA expression levels.

3. Results

3.1. The timing of the neurogenesis to gliogenesis transition of spinal cord NSC is preserved in vitro

Neurospheres were used to evaluate the temporal association between cell cycle lengthening and the loss of the NSC neurogenic potential. In the cervical spinal cord, neurogenesis progresses through days 10–14 of embryonic development (Nornes and Carry, 1978). We then compared the neurogenic/gliogenic potential of neurospheres from a neurogenic stage, embryonic day 11 (E11), a transition stage, embryonic day 14 (E14) and a gliogenic stage, postnatal day 1 (P1). The differentiation potential was assessed by double immunostaining with MAP2, a neuron marker, and GFAP, a marker of astrocytes. Given that each cellular aggregate is the result of clonal divisions (Suslov et al., 2002), quantifying the proportion of neurospheres that were formed mostly by neurons, mostly by astrocytes or by a mixed population of neurons and astrocytes, allows the assessment of the heterogenic differentiation potential of the parental cells that were obtained from each stage. As shown in Fig. 1, almost 60% of neurospheres obtained from E11 displayed MAP2 immunoreactivity. A similar proportion of E14 neurospheres gave rise to either MAP2 or GFAP positive cells. Lastly, P1 neurospheres preferentially originated GFAP positive cells. The neurospheres illustrated on Fig. 1A represent the most abundant profile of each stage of development.

3.2. Neurogenic NSC divide faster and display shorter cell cycle duration

At first glance, neurospheres reduced their sizes from E11 to P1 (Figs. 1 and 2A). Reduction in neurosphere size has been associated to a decrease in the self-renewal potential of NSCs that is not associated with an increase of cell death, but to a reduced proliferation (Molofsky et al., 2003); thus we decided to test if proliferation decreases, and the cell cycle length increases, as the developmental time progressed. Cumulative BrdU labeling allows the assessment of changes in NSC proliferation rate; we used this technique to estimate changes in the duration of the cell cycle during development. The number of BrdU labeled cells was significantly higher in E11 neurospheres than in E14 and P1 neurospheres (Fig. 2B). The regression analysis conducted to estimate cell cycle length based on BrdU cumulative data revealed that E11 NSC cycle lasts 34.7 h, whereas that for E14 and PD1 NSC spans 51.4 and 52.8 h respectively. Hence, the neurogenesis to gliogenesis transition encompasses a lengthening of NSC cell cycle and a decay of the proliferation rate.

3.3. NSC expression of CKI increase during the transition to the gliogenic phase

CKI participate in the control of cell proliferation and cell cycle length, as well as in the modulation of the cell cycle length during the onset of the gliogenic phase in telencephalic structures (Nagao et al., 2008). Then, mRNA expression levels of $p27^{Kip}$, $p21^{Cip}$, $p19^{INK4D}$, $p16^{INK4A}$ and $p19^{ARF}$, prominent members of the Cip/Kip and INK4 CKI families, respectively, were estimated in E11, E14 and P1 spinal cord neurospheres. As seen in Fig. 3, there seemed to be an increased expression of $p21^{Cip}$ mRNA on E14 and P1 neurospheres, but not of $p27^{Kip}$, nor $p19^{INK4D}$; nevertheless, this was not a statistically significant increase ($p > 0.05$). $p16^{INK4A}$ mRNA expression was not consistently detected. A significant increased expression was observed for $p19^{ARF}$, and because of it, we reasoned p53 could be involved in the regulation of the NSC proliferation and cell cycle length during the transition from the neurogenic to the gliogenic phase. Even though high levels of the p53 mRNA expression were observed at all time points, its levels were comparable among E11, E14 and P1 neurospheres (Fig. 3).

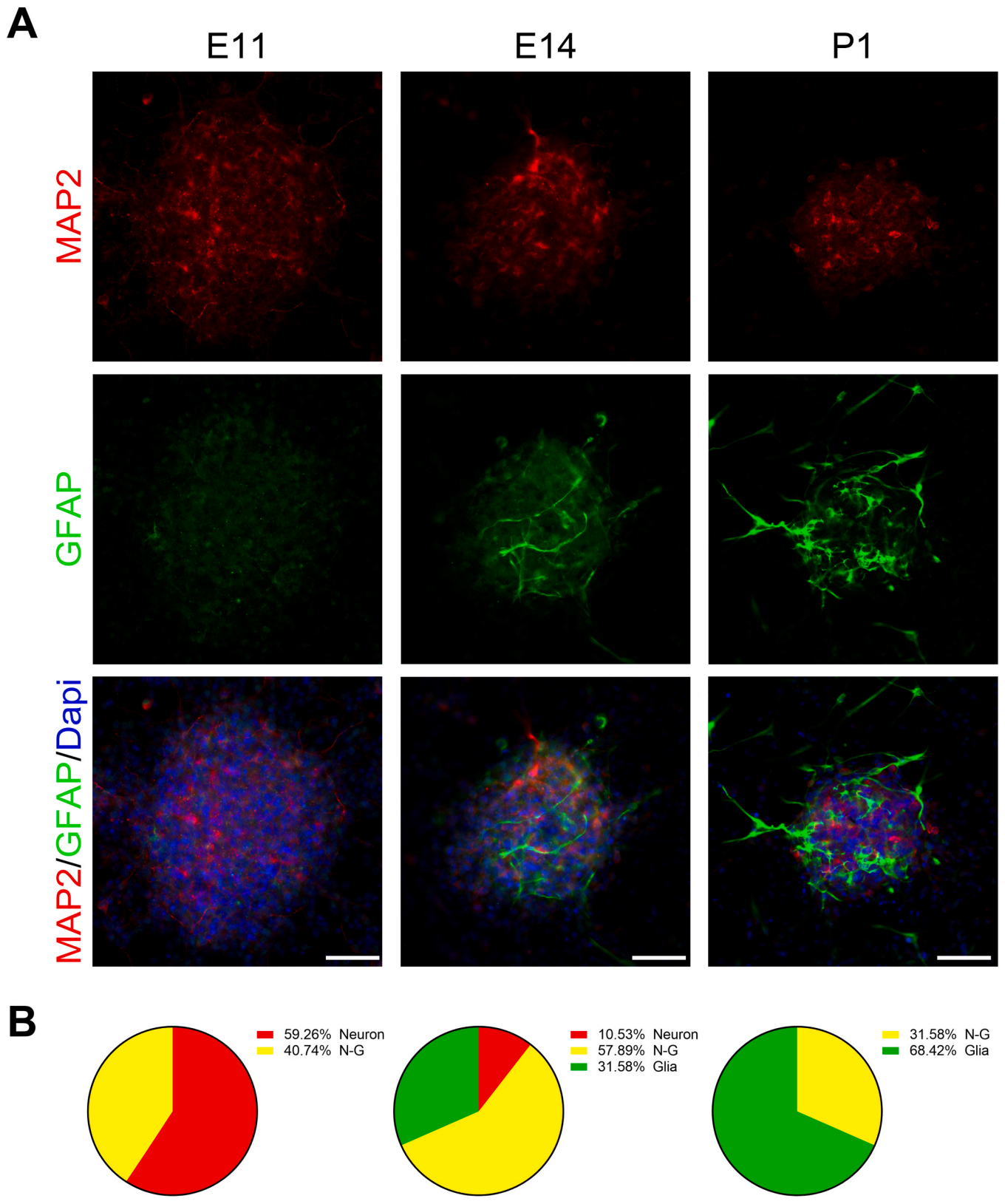

Fig. 1. Embryonic spinal cord neurospheres recapitulate timely the neurogenesis to gliogenesis transition reported in vivo. A) Fluorescence photomicrographs showing one secondary neurosphere from E11, E14 and P1 cultures, stained for MAP2 and GFAP, and counterstained with DAPI. Scale bar: 100 μm. B) Quantification of the proportion of neurospheres that were formed mostly by neurons, mostly by astrocytes or by a mixed population of neurons and astrocytes on the secondary neurosphere cultures from each stage of development.

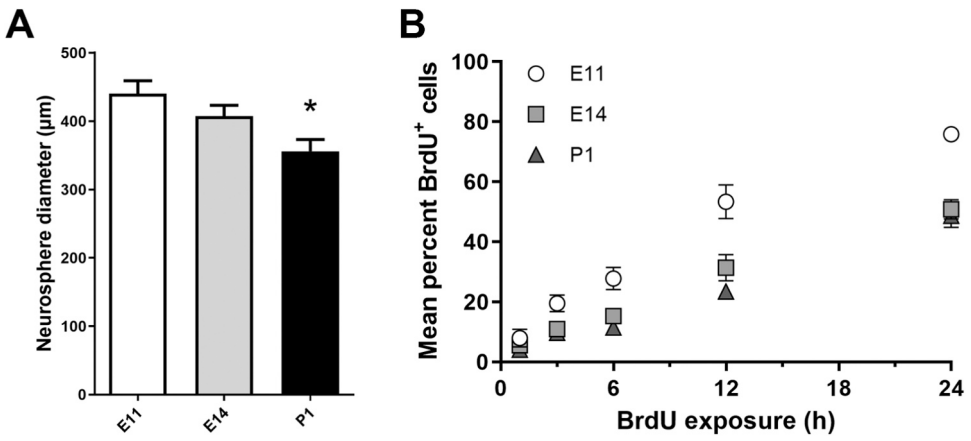

Fig. 2. Embryonic spinal cord NSC proliferation drops and cell cycle lengthens during development. A) Bar graph displaying the average diameter of E11, E14 and P1 neurospheres. Data are presented as mean + SEM. *p = 0.0021. E11 = 439.9 + 18.94 (n = 43); E14 = 407 + 15.95 (n = 28); P1 = 355.5 + 17.47 (n = 40). B) Dot graph depicting the time-course of cumulative BrdU labeling in E11, E14 and P1 neurospheres. Data are presented as mean ± SEM.

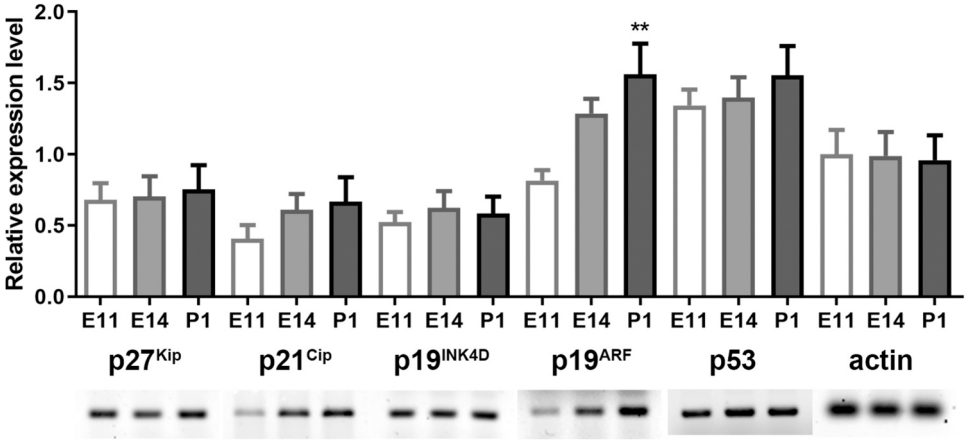

Fig. 3. Members of the Cip/Kip and INK4 CKI families accumulate in spinal cord NSC during de neurogenesis to gliogenesis transition phase. Bar graph that depicts the relative expression levels of CKI in E11, E14 and P1 spinal cord neurospheres. The photographs aligned bellow the graph illustrate representative bands for each CKI analyzed at different age. Data are presented as mean ± SEM. **p = 0.0048.

3.4. Olomoucine affects the proliferation rate but not the differentiation potential of E11 neurospheres

So far, our results support the idea that the loss of the neurogenic potential of spinal cord NSC during the neurogenesis to gliogenesis transition is associated with increments of the expression of key CKI that might reduce NSC proliferation rate by lengthening the cell cycle. This notion was further evaluated by exposing E11 neurogenic neurospheres to Olomoucine, a specific inhibitor of CDK that lengthen the G1 phase progression. Accordingly, the size of Olomoucine-treated, E11 neurospheres was significantly smaller than that documented for untreated E11 neurospheres (Fig. 4A). We quantified again the proportion of neurospheres that were formed mostly by neurons, mostly by astrocytes or by a mixed population of neurons and astrocytes, to assess the effect of the olomoucine treatment on the differentiation potential of the cells obtained from the E11 spinal cord. DMSO treated cultures gave rise to neurospheres formed mostly by neurons and formed by neurons and astrocytes; the percentage difference with the non-treated culture (Fig. 1B) was not significant (according to a chi-square test). Despite the effect on size, the proportion of neurospheres MAP2 positive cells did not change with the Olomoucine treatment (Fig. 4B and C), suggesting that the intracellular mechanisms that regulate the gliogenesis onset are independent of the cell cycle progression. The neurospheres illustrated on Fig. 4C represent the most abundant profile of each treatment; it was surprising to find small neurospheres mostly formed by neurons because the similar size neurospheres from P1 cultures (Fig. 1A) were mostly formed by astrocytes.

4. Discussion

The mechanisms underlying the restriction of the neurogenic potential of embryonic NSC remain unclear. The fact that this constraint coincides with the onset of glial cell generation suggests that the molecular processes governing the transition from the neurogenic to the gliogenic phase might be involved. Accordingly, it has been established that the imbalance of pro-neuronal/anti-glial and/or anti-neuronal/pro-glial transcription factors and of their associated second messenger signaling cascades influence NSC commitment to one or the other phenotype (Christie et al., 2013). Multiple efforts have been made to understand lineage determination in the CNS, there is a clear biomedical need to gain control over cell fate and to be able of directing neuronal differentiation (Grade and Götz, 2017; Ninkovic and Götz, 2013); unfortunately these studies have focused mainly on NSC from the brain and we believe the spinal cord population should also be characterized. Data generated in this study shows that mechanisms that had been described for telencephalic NSC might be different in the spinal cord.

The relevance of gene expression for neurogenesis has been established by transcriptional profiling telencephalic NSC (Azim et al., 2018;

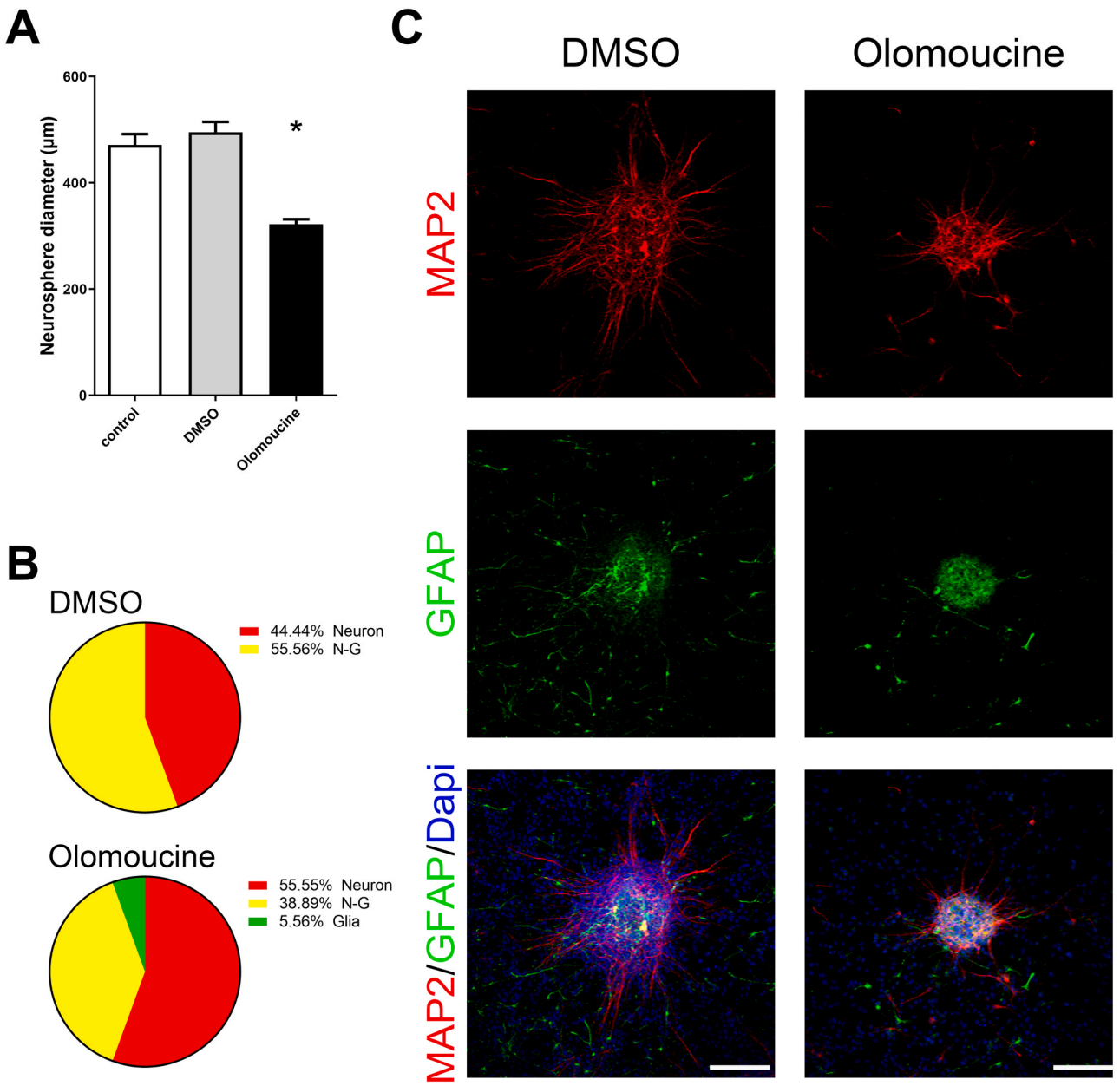

Fig. 4. Olomoucine effect on proliferation and differentiation. A) Bar graph displaying the average diameter of untreated, DMSO-exposed and Olomoucine treated E11 neurospheres. Data are presented as mean + SEM. *p = 0.0001 Control = 471.3 + 20.37 (n = 68); DMSO = 495.4 + 19.48 (n = 58); Olomoucine = 322 + 9.665 (n = 63). B) Quantification of the proportion of neurospheres that were formed mostly by neurons, mostly by astrocytes or by a mixed population of neurons and astrocytes. C) Fluorescence photomicrographs showing DMSO exposed or Olomoucine treated E11 neurospheres stained for MAP2 and GFAP, and counterstained with DAPI. Scale bar: 100 µm.

Jones and Connor, 2016) but some studies have also suggested the existence of an association between the restriction of the differentiation potential and the molecular machinery that controls the cell cycle progression and length. For instance, chromatin remodeling ongoing during cell cycle progression influences cell fate (Ma et al., 2015). Also, the shortening of the G1 phase and thus a faster proliferation rate, both restrict pluripotency of embryonic stem cells (Coronado et al., 2013). Our results in embryonic spinal cord NSC, however, suggest otherwise. We found that the loss of NSC neurogenic potential during the neurogenic to gliogenic transition phase is independent from the reduction of NSC proliferation rate, the latter being inferred by the observed increments of the expression of cell cycle regulators, known to decrease it, and the reduction of the BrdU cumulative labeling. Further support to our conclusion comes from the fact that Olomoucine treated-neurospheres showed reduced proliferation rates and sizes, without losing their neurogenic potential.

The proliferation kinetics of NSC isolated from the spinal cord are not easy to compare to the ones from telencephalic cells; cell cycle parameters that have been used for cortical cells (Takahashi et al., 1993) are not possible to calculate given that the quantification of BrdU accumulation does not reach the curve plateau in 24 h; this feature resemble the BrdU labeling of telencephalic neurospheres from 480-days old mice (Kippin et al., 2005); nevertheless, the analysis within the 24-h window is sufficient to show that neurogenic cells divide faster than those generating glia. We also found cell cycle regulators in our spinal cord model that have not been shown in telencephalic models; for example, in telencephalic NSC, $p16^{INK4A}$ has been described as effector of the Bmi1 transcription factor to regulate cell self-renewal (Molofsky et al., 2003);

we were not able to measure this molecule consistently and, instead, we found the other Bmi1 regulated molecule, $p19^{ARF}$, significantly increased in P1 spinal cord neurospheres. All this strengthen the idea that it is necessary to go further on the spinal cord characterization.

Previous studies suggest that lengthening or shortening the cell cycle of telencephalic NSC delays or onwards neurogenesis (Calegari and Huttner, 2003; Lange et al., 2009). It is presumed that a lengthier cell cycles makes susceptible NSC to extracellular influences. In contrast, our results support that this might not be the case on NSC going through the neurogenic/gliogenic transition phase. Since Olomoucine did reduce NSC proliferation rates, thus shortening cell cycle length, without altering NSC neurogenic potential, our observations support that NSC coursing through the neurogenic/gliogenic transition phase may be less susceptible to be modulated by extrinsic signals. This possibility agrees with data that highlights the relevance of intrinsic differences between subpopulations of NSC that affect their neurogenic potential (Seaberg et al., 2005).

The ultimate restriction of stem cells' differentiation potential is commonly associated to cell cycle arrest and senescence, even though stem cells display a variety of mechanisms to evade them for some time (reviewed by Schultz and Sinclair (2016)). That stem cells senesce is clearly shown by a variety of indicators among of which the accumulation of cell cycle inhibitors as senescence markers, like $p16^{INK4A}$, are paramount. The expression of cell cycle inhibitors and the lengthening of the cell cycle observed in embryonic spinal cord NSC in our experimental series suggest that senescence might also be part of the ontogeny of the nervous system, as suggested for other embryonic tissues (Muñoz-Espín et al., 2013; Storer et al., 2013). If this was the case, the irreversibility of the changes in the cellular homeostasis associated with the senescence establishment, might be the explanation to the loss of the neurogenic potential of NSC. Estimating telomere length and beta-galactosidase activity during the transition from neurogenesis to gliogenesis could shed light into this important matter.

Funding

Financial support was provided by the Instituto de Investigaciones Biomédicas, Universidad Nacional Autónoma de México and project IMPULSA 02 from Coordinación de la Investigación Científica, Universidad Nacional Autónoma de México. LOC received fellowship 210327 from Consejo Nacional de Ciencia y Tecnología (CONACyT), Mexico.

Compliance with Ethical Standards

We further confirm that any aspect of the work covered in this manuscript that has involved experimental animals has been conducted with the ethical approval of the Animal Rights Committee at Instituto de Investigaciones Biomédicas, Universidad Nacional Autónoma de México.

Author contributions

Conceptualization and design of the study: LOC, GGO. Acquisition of data: LOC, JRS. Analysis and interpretation of data: All authors. Drafting of the manuscript: LOC and GGO. Critical review of manuscript: All authors. Approval of final manuscript: All authors.

CRediT authorship contribution statement

Leonora Olivos-Cisneros: Conceptualization. **Gabriel Gutiérrez-Ospina:** Conceptualization.

Conflict of Interest

The authors declare that there are no known conflicts of interest associated with this publication and there has been no significant financial support for this work that could have influenced its outcome.

Acknowledgments

Authors thank Miguel Tapia-Rodríguez and Georgina Diaz-Herrera for technical support. Leonora Olivos-Cisneros is a Ph.D. student at Programa de Doctorado en Ciencias Biomédicas, Universidad Nacional Autónoma de México; the work reported in this manuscript is part of her doctoral dissertation.

References

Azim, K., Akkermann, R., Cantone, M., Vera, J., Jadasz, J.J., Küry, P., 2018. Transcriptional profiling of ligand expression in cell specific populations of the adult mouse forebrain that regulates neurogenesis. Front. Neurosci. 12. https://doi.org/10.3389/fnins.2018.00220.

Bottari, N.B., Schetinger, M.R.C., Pillat, M.M., Palma, T.V., Ulrich, H., Alves, M.S., Morsch, V.M., Melazzo, C., de Barros, L.D., Garcia, J.L., Da Silva, A.S., 2019. Resveratrol as a therapy to restore neurogliogenesis of neural progenitor cells infected by Toxoplasma gondii. Mol. Neurobiol. 56, 2328–2338. https://doi.org/10.1007/s12035-018-1180-z.

Calegari, F., Huttner, W.B., 2003. An inhibition of cyclin-dependent kinases that lengthens, but does not arrest, neuroepithelial cell cycle induces premature neurogenesis. J. Cell Sci. 116, 4947–4955. https://doi.org/10.1242/jcs.00825.

Christie, K.J., Emery, B., Denham, M., Bujalka, H., Cate, H.S., Turnley, A.M., 2013. Transcriptional regulation and specification of neural stem cells. Transcr. Transl. Regul. Stem Cells 129–155. https://doi.org/10.1007/978-94-007-6621-1_8.

Coronado, D., Godet, M., Bourillot, P.-Y., Tapponnier, Y., Bernat, A., Petit, M., Afanassieff, M., Markossian, S., Malashicheva, A., Iacone, R., Anastassiadis, K., Savatier, P., 2013. A short G1 phase is an intrinsic determinant of naïve embryonic stem cell pluripotency. Stem Cell Res. 10, 118–131. https://doi.org/10.1016/j.scr.2012.10.004.

Fracasso, M., Pillat, M.M., Bottari, N.B., da Silva, A.D., Grando, T.H., Matos, A.F.I.M., Petry, L.S., Ulrich, H., de Andrade, C.M., Monteiro, S.G., Da Silva, A.S., 2019. Trypanosoma evansi impacts on embryonic neural progenitor cell functions. Microb. Pathog. 136, 103703 https://doi.org/10.1016/j.micpath.2019.103703.

Grade, S., Götz, M., 2017. Neuronal replacement therapy: previous achievements and challenges ahead. npj Regen. Med. 2. https://doi.org/10.1038/s41536-017-0033-0.

Gui, H., Li, S., Matise, M.P., 2007. A cell-autonomous requirement for Cip/Kip cyclin-kinase inhibitors in regulating neuronal cell cycle exit but not differentiation in the developing spinal cord. Dev. Biol. 301, 14–26. https://doi.org/10.1016/j.ydbio.2006.10.035.

He, S., Iwashita, T., Buchstaller, J., Molofsky, A.V., Thomas, D., Morrison, S.J., 2009. Bmi-1 over-expression in neural stem/progenitor cells increases proliferation and neurogenesis in culture but has little effect on these functions in vivo. Dev. Biol. 328, 257–272. https://doi.org/10.1016/j.ydbio.2009.01.020.

Jones, K.S., Connor, B.J., 2016. The effect of pro-neurogenic gene expression on adult subventricular zone precursor cell recruitment and fate determination after excitotoxic brain injury. J. Stem Cells Regen. Med. 12, P25–P35.

Kicheva, A., Bollenbach, T., Ribeiro, A., Valle, H.P., Lovell-Badge, R., Episkopou, V., Briscoe, J., 2014. Coordination of progenitor specification and growth in mouse and chick spinal cord. Science 345, 1254927. https://doi.org/10.1126/science.1254927.

Kippin, T.E., Martens, D.J., Van Der Kooy, D., 2005. P21 loss compromises the relative quiescence of forebrain stem cell proliferation leading to exhaustion of their proliferation capacity. Genes Dev. 19, 756–767. https://doi.org/10.1101/gad.1272305.

Lange, C., Huttner, W.B., Calegari, F., 2009. Cdk4/CyclinD1 overexpression in neural stem cells shortens G1, delays neurogenesis, and promotes the generation and expansion of basal progenitors. Cell Stem Cell 5, 320–331. https://doi.org/10.1016/j.stem.2009.05.026.

Ma, Y., Kanakousaki, K., Buttitta, L., 2015. How the cell cycle impacts chromatin architecture and influences cell fate. Front. Genet. 5, 1–18. https://doi.org/10.3389/fgene.2015.00019.

Martens, D.J., Seaberg, R.M., Van Der Kooy, D., 2002. In vivo infusions of exogenous growth factors into the fourth ventricle of the adult mouse brain increase the proliferation of neural progenitors around the fourth ventricle and the central canal of the spinal cord. Eur. J. Neurosci. 16, 1045–1057. https://doi.org/10.1046/j.1460-9568.2002.02181.x.

Miller, F.D., Gauthier, A.S., 2007. Timing is everything: making neurons versus glia in the developing cortex. Neuron 54, 357–369. https://doi.org/10.1016/j.neuron.2007.04.019.

Molofsky, A.V., Pardal, R., Iwashita, T., Park, I.-K., Clarke, M.F., Morrison, S.J., 2003. Bmi-1 dependence distinguishes neural stem cell self-renewal from progenitor proliferation. Nature 425, 962–967. https://doi.org/10.1038/nature02060.

Muñoz-Espín, D., Cañamero, M., Maraver, A., Gómez-López, G., Contreras, J., Murillo-Cuesta, S., Rodríguez-Baeza, A., Varela-Nieto, I., Ruberte, J., Collado, M., Serrano, M., 2013. Programmed cell senescence during mammalian embryonic development. Cell 155. https://doi.org/10.1016/j.cell.2013.10.019.

Nagao, M., Campbell, K., Burns, K., Kuan, C.-Y., Trumpp, A., Nakafuku, M., 2008. Coordinated control of self-renewal and differentiation of neural stem cells by Myc

and the p19 ARF –p53 pathway. J. Cell Biol. 183, 1243–1257. https://doi.org/10.1083/jcb.200807130.
Ninkovic, J., Götz, M., 2013. Fate specification in the adult brain - lessons for eliciting neurogenesis from glial cells. BioEssays 35, 242–252. https://doi.org/10.1002/bies.201200108.
Nornes, H.O., Carry, M., 1978. Neurogenesis in spinal cord of mouse: an autoradiographic analysis. Brain Res. 159, 1–16. https://doi.org/10.1016/0006-8993(78)90105-1.
Qian, X., Shen, Q., Goderie, S.K., He, W., Capela, A., Davis, A.A., Temple, S., 2000. Timing of CNS cell generation: a programmed sequence of neuron and glial cell production from isolated murine cortical stem cells. Neuron 28, 69–80.
Ruddy, R.M., Morshead, C.M., 2018. Home sweet home: the neural stem cell niche throughout development and after injury. Cell Tissue Res. 371, 125–141. https://doi.org/10.1007/s00441-017-2658-0.
Schultz, M.B., Sinclair, D.A., 2016. When stem cells grow old: phenotypes and mechanisms of stem cell aging. Development 143, 3–14. https://doi.org/10.1242/dev.130633.
Seaberg, R.M., Smukler, S.R., Van Der Kooy, D., 2005. Intrinsic differences distinguish transiently neurogenic progenitors from neural stem cells in the early postnatal brain. Dev. Biol. 278, 71–85. https://doi.org/10.1016/j.ydbio.2004.10.017.
Storer, M., Mas, A., Robert-Moreno, A., Pecoraro, M., Ortells, M.C., Di Giacomo, V., Yosef, R., Pilpel, N., Krizhanovsky, V., Sharpe, J., Keyes, W.M., 2013. Senescence is a developmental mechanism that contributes to embryonic growth and patterning. Cell 155, 1119–1130. https://doi.org/10.1016/j.cell.2013.10.041.
Suslov, O.N., Kukekov, V.G., Ignatova, T.N., Steindler, D.A., 2002. Neural stem cell heterogeneity demonstrated by molecular phenotyping of clonal neurospheres. Proc. Natl. Acad. Sci. USA 99, 14506–14511. https://doi.org/10.1073/pnas.212525299.
Takahashi, T., Nowakowski, R.S., Caviness, V.S., 1993. Cell cycle parameters and patterns of nuclear movement in the neocortical proliferative zone of the fetal mouse. J. Neurosci. 13, 820–833. https://doi.org/10.1523/jneurosci.13-02-00820.1993.
Temple, S., 2006. Defining neural stem cells and their role in normal development of the nervous system. In: Rao, Mahendra S. (Ed.), Neural Development and Stem Cells. Humana Press, Totowa, NJ, pp. 1–28. https://doi.org/10.1385/1-59259-914-1:001.
Whittemore, S.R., Morassutti, D.J., Walters, W.M., Liu, R.H., Magnuson, D.S.K., 1999. Mitogen and substrate differentially affect the lineage restriction of adult rat subventricular zone neural precursor cell populations. Exp. Cell Res. 252, 75–95. https://doi.org/10.1006/excr.1999.4621.